J. Fluid Mech. (2005), *vol.* 545, *pp.* 427–443.
doi:10.1017/S0022112005006853 Printed in the United Kingdom

An over-pressure correction to the slug model for vortex ring circulation

By PAUL S. KRUEGER

Department of Mechanical Engineering, Southern Methodist University, Dallas, TX 75275, USA

(Received 8 June 2004 and in revised form 20 June 2005)

The slug model provides a formula for the circulation of vortex rings formed by starting jets ejected from a nozzle or orifice in terms of the time history of the jet velocity. For rapidly initiated jets, however, the model under-predicts circulation by an amount that remains nearly constant as circulation increases. To remedy this shortcoming, the present study derives an equation for circulation directly from the governing equations for the flow, illustrating that the circulation can be expressed as the sum of a flux term, Γ_U, determined by the jet centreline velocity and a 'source' term, Γ_p, determined by over-pressure at the jet centreline during vortex ring formation. For impulsively or nearly impulsively initiated jets, Γ_p is modelled using potential flow analysis since over-pressure is significant primarily during the rapid jet initiation in these cases. The effects of the jet initiation and boundary-layer growth on the jet centreline velocity are also considered to provide a realistic model for Γ_U. Models for nozzle and orifice configurations are developed. In the case of a nozzle-type generator, the need to model the jet centreline velocity leads to an approximate solution for starting flow near the exit of an infinitely long pipe. For the nozzle case, the model results agree with available circulation measurements to within $\pm 6.2\,\%$ for a wide range of conditions, except for jet velocity programs that are nearly triangular. In the orifice case, the model agrees with available results to within $-13\,\%$. Both cases show substantial improvement over the slug model, which is in error by $-21\,\%$ to $-67\,\%$ for the data considered.

1. Introduction

The sudden ejection of a jet from a nozzle or orifice is a frequently observed unsteady flow. It is a distinguishing feature of many important systems ranging from aquatic propulsion of squid and salps (Siekmann 1963; Weihs 1977) to synthetic jet actuators (Glezer & Amitay 2002). A piston–cylinder mechanism is commonly used to study such flows in the laboratory (Shuster & Smith 2004, Anderson & Grosenbaugh 2005). Two common incarnations of this mechanism are the nozzle and orifice configurations, with geometries defined in figure 1. To generate the desired flow, the piston is moved at a specified velocity $U_p(t)$ for a finite duration t_p, thereby ejecting a jet of velocity $U_J(t)$ and length $L = \int_0^{t_p} U_J(t)\,\mathrm{d}t$ into the surrounding fluid. The jet velocity $U_J(t)$ is related to the piston velocity $U_p(t)$ through continuity, as indicated in the caption for figure 1. During the piston motion, the boundary layer developing inside the device separates at the nozzle/orifice lip. The result is a cylindrical sheet of vorticity that rolls up into a vortex ring as it is being ejected (Didden 1979; Nitsche & Krasny 1994; Nitsche 1996).

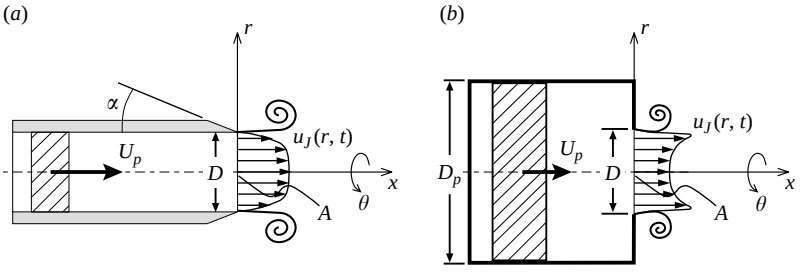

FIGURE 1. Schematic of (*a*) nozzle and (*b*) orifice type piston–cylinder vortex ring generators. (*a*) $U_J(t) = U_P(t)$. (*b*) $U_J(t) = (D_P/D)^2 U_P(t)$.

While vortex rings themselves have been studied in a variety of situations (see the reviews by Shariff & Leonard 1992; Lim & Nickels 1995), increased attention has recently been given to the vortex-ring formation process. A focus on ring formation is motivated by the fundamental importance of the formation process for performance and behaviour of highly unsteady jets in applications related to propulsion (Krueger & Gharib 2003, 2005) and flow control using synthetic jet actuators (Shuster & Smith 2004). In this regard, it is desirable to know how the basic parameters of the formation process affect the properties of the resulting vortex ring (or rings) so that the flow may be manipulated as desired. Specifically, we would like to predict the properties of the resulting vortex ring, given the geometry of the generator and the piston velocity program, $U_p(t)$.

An important set of vortex-ring properties is the invariants of motion, namely, the ring kinetic energy, impulse and circulation (Mohseni & Gharib 1998). Of these three, the ring circulation, Γ, is the simplest to measure experimentally and, perhaps, the easiest to relate to the formation process. Several models have been proposed for determining Γ (dating back to Sallet 1975), but the most common model used for vortex rings formed by a piston–cylinder mechanism is the so-called 'slug model'.

The slug model estimates the vortex-ring circulation as

$$\Gamma_{sm} = \frac{1}{2}\int_0^{t_p} U_J^2(t)\,\mathrm{d}t \tag{1}$$

(Glezer 1988; Shariff & Leonard 1992) where the subscript '*sm*' is used herein to denote the slug-model prediction. Although the slug model has been used extensively in previous investigations, it is worth outlining the theoretical basis of the slug model to facilitate the present discussion. For flow with zero swirl, the slug model assumes that the flux of vorticity across the jet exit plane is $u\omega_\theta|_{x=0}$, in which case the rate of change of circulation in the flow is

$$\frac{\partial \Gamma}{\partial t} = \int_0^{\infty} u\omega_\theta|_{x=0}\,\mathrm{d}r \tag{2}$$

(Didden 1979). Invoking the parallel flow assumption (namely, that the radial flow velocity, v, at the nozzle/orifice exit is zero for all time), the azimuthal vorticity is approximated by $\omega_\theta \approx -\partial u/\partial r$ and equation (2) integrates to

$$\frac{\partial \Gamma}{\partial t} \approx \tfrac{1}{2}u_{cl}^2(t), \tag{3}$$

where $u_{cl}(t)$ is the centreline velocity at the jet exit plane. Making the additional assumption of uniform axial velocity at the jet exit (i.e. slug flow) so that $u_{cl}(t) \approx U_J(t)$ and integrating in time gives equation (1).

Numerous experimental and numerical studies have observed that the slug model under-predicts the ring circulation (e.g. Didden 1979; Nitsche & Krasny 1994; James & Madnia 1996; Heeg & Riley 1997; Weigand & Gharib 1997; Gharib, Rambod & Shariff 1998; Rosenfeld, Rambod & Gharib 1998; Zhao, Frankel & Mongeau 2000). Among these, the experiments of Didden (1979) are notable as the first to measure the flow velocity at the jet exit plane, and thereby relate the vorticity flux during the formation process to the circulation of the resulting vortex ring. Using a nozzle configuration (small α) in water, Didden observed that the absolute error in the slug model was nearly constant for all L/D tested (from 0.6 to 2.2). This conclusion seemed relatively independent of the ring Reynolds number, $Re_\Gamma \equiv \Gamma/\nu$, which fell in the range 980–2800. The absolute error was substantial (more than 20 % of the total circulation for the conditions tested). Didden attributed the failure of the model primarily to non-uniform flow near the nozzle lip during the initiation of the pulse (the jet axial velocity, $u_J(r, t)$, near the nozzle lip exceeded the piston velocity during initiation of the flow). Factors affecting the model accuracy to a lesser degree were boundary-layer growth causing u_{cl} to increase above U_J for large L/D (which contributes to an under-prediction of Γ by the slug model), and entrainment of negative vorticity into the ring as the ring rolls up around the outer annulus of the nozzle (which contributes to an over-prediction of Γ by the slug model).

Significantly, Didden's results indicate that the offset between the actual circulation and the slug-model prediction occurs during the initiation of the piston motion, which was characterized by a rapid acceleration to a velocity $U_0 = 4.6\,\mathrm{cm\,s^{-1}}$, where it remained for the duration of the pulse. The recent numerical investigations of James & Madnia (1996) and Heeg & Riley (1997) confirmed this observation and demonstrate that $\partial\Gamma/\partial t$ obtains a local maximum during flow initiation that is well above the circulation flux predicted by the slug model. If the initial flow acceleration is increased, the magnitude of the initial peak in $\partial\Gamma/\partial t$ increases, but the period over which $\partial\Gamma/\partial t$ is above the slug-model value decreases. Following the initial transient, James & Madnia showed near exact agreement between $\partial\Gamma/\partial t$ computed in their simulations and that predicted by the slug model since they specify a nearly flat velocity profile at the jet exit plane ($U_J \approx u_{cl} = \text{constant}$). Heeg & Riley, on the other hand, showed $\partial\Gamma/\partial t$ slightly above the slug model value at large time owing to boundary-layer growth inside the nozzle.

These results demonstrate that error in the slug model arises primarily from events related to the initiation of the flow for rapidly initiated piston motion. As first expressed by Didden (1979), the discrepancy during flow initiation is related to the peak in jet axial velocity u_J that develops near the nozzle lip during the acceleration of the piston. Nevertheless, the shortcomings of the slug model cannot be expressed entirely in terms of a peak in u_J near the nozzle lip without regard to the radial velocity v since the circulation flux due to u_J alone (with $v = 0$) depends only on u_{cl}, as shown in equation (3). Rather, the peak in u_J near the nozzle lip is significant because Didden (1979) shows a peak in $\partial v/\partial x$ (the v contribution to ω_θ) nearly coincident with the initial peak in u_J, indicating that $\partial v/\partial x$ provides a significant contribution to the flux of circulation at early time. The behaviour of u_J and $\partial v/\partial x$ can both be related to over-pressure at the nozzle exit plane, which develops as a result of the unsteady flow initiation and distorts the velocity profile at the nozzle. The present

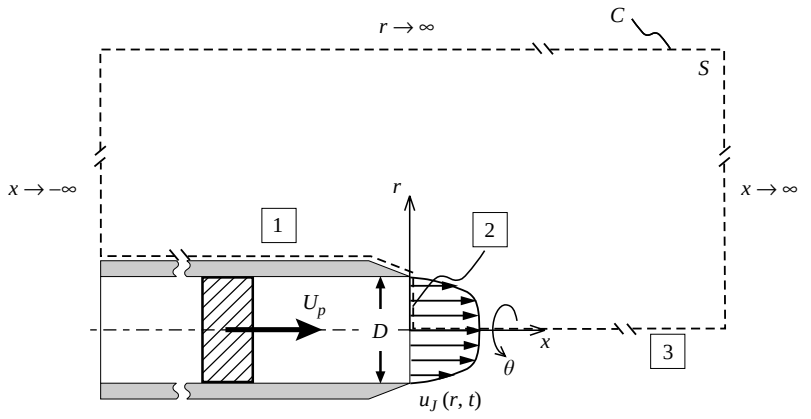

FIGURE 2. A surface S and bounding contour C for determining the rate at which circulation is injected into the fluid by a piston–cylinder mechanism.

effort seeks to model the over-pressure effect, demonstrating how it affects the flux of vorticity and providing a correction to the slug model.

2. An equation for total circulation and its application to a piston–cylinder mechanism

The effect of over-pressure on the flux of vorticity during vortex-ring formation can be obtained best by deriving an equation for circulation from the vorticity transport equation in incompressible flow, namely,

$$\frac{\partial \boldsymbol{\omega}}{\partial t} + \nabla \times (\boldsymbol{\omega} \times \boldsymbol{u}) = -\nu \nabla \times (\nabla \times \boldsymbol{\omega}). \tag{4}$$

Integrating equation (4) over an arbitrary surface S with bounding contour C and applying Stoke's theorem gives

$$\frac{\partial \Gamma}{\partial t} = -\oint_C (\boldsymbol{\omega} \times \boldsymbol{u} + \nu \nabla \times \boldsymbol{\omega}) \cdot \mathrm{d}\boldsymbol{c}, \tag{5}$$

where $\Gamma = \int_S \boldsymbol{\omega}(\boldsymbol{x}, t) \cdot \hat{\boldsymbol{n}}\, \mathrm{d}S$ and $\hat{\boldsymbol{n}}$ is the outward normal to S. Using the incompressible momentum equation to substitute for $\nu \nabla \times \boldsymbol{\omega}$ yields the alternative form

$$\frac{\partial \Gamma}{\partial t} = -\oint_C \left[\boldsymbol{\omega} \times \boldsymbol{u} - \left(\frac{\mathrm{D}\boldsymbol{u}}{\mathrm{D}t} + \frac{\nabla \tilde{p}}{\rho} \right) \right] \cdot \mathrm{d}\boldsymbol{c}, \tag{6}$$

where the hydrostatic pressure distribution has been absorbed into $\tilde{p}$ so that $\tilde{p} \to 0$ as $|\boldsymbol{x}| \to \infty$. Equation (5) or (6) allows determination of the rate of change of circulation in a fixed open area using flow quantities on the perimeter of the area. The $\boldsymbol{\omega} \times \boldsymbol{u}$ term represents a flux of vorticity across C, but the $\mathrm{D}\boldsymbol{u}/\mathrm{D}t$ and $\nabla \tilde{p}/\rho$ terms are vorticity 'sources'.

To apply the above results to the flow generated by a piston–cylinder mechanism, an appropriate contour is a planar contour that intersects the axis of the generator, such as the contour depicted in figure 2. Figure 2 illustrates the special case of a nozzle configuration, but the following analysis holds for an orifice configuration as well. Using the contour in figure 2, the integrals for either equation (5) or (6) are zero along the portions at infinity since the integrands decay as $|\boldsymbol{x}|^{-n}$, $n > 2$, for large

$|\boldsymbol{x}|$ (Cantwell 1986). Furthermore, using equation (5) the contour integral along the centreline (segment 3 in figure 2) reduces to

$$-\nu \int_0^\infty \frac{1}{r} \frac{\partial (r\omega_\theta)}{\partial r}\bigg|_{r\to 0} \mathrm{d}x$$

after invoking axisymmetry. This integral is related to the diffusion of vorticity across the centreline, which may be neglected as long as ω_θ is zero in some neighbourhood of $r = 0$ (or $\omega_\theta \sim O(r^n)$ for $n > 1$ as $r \to 0$). Since the vorticity from the boundary layer and forming ring diffuse a distance $O(\sqrt{\nu t})$ in a time t, a sufficient condition for ignoring the integral along the centreline is $\sqrt{\nu t}_p \ll D/2$. Equivalently,

$$\frac{t_p U_0}{D} \ll Re_0 \quad \text{or} \quad \frac{L}{D} \ll Re_0, \tag{7}$$

where $Re_0 = U_0 D/\nu$ is the jet Reynolds number based on the maximum velocity during the pulse, U_0, and $L \sim U_0 t_p$ for jet velocity programs of interest (see § 3).

Provided equation (7) is satisfied, the contour integral for $\partial \Gamma/\partial t$ is completely determined by the integrals along the nozzle exit plane and the outer annulus of the cylinder (segments 2 and 1, respectively, in figure 2). Integrating equation (6) along the remaining portion of the contour and using appropriate boundary conditions gives

$$\frac{\partial \Gamma}{\partial t} = \tfrac{1}{2} u_{cl}^2(t) + \frac{1}{\rho} \tilde{p}_{cl}(t) - \frac{\partial}{\partial t} \int_0^{D/2} v|_{x=0} \, \mathrm{d}r, \tag{8}$$

where u_{cl} and $\tilde{p}_{cl}$ are the axial velocity and pressure, respectively, at $(x, r) = (0, 0)$. In obtaining equation (8), it was observed that the velocity components are zero along the outer annulus of the nozzle by the no-slip condition, but the pressure term in equation (6) may not be zero on the outer annulus and must be integrated out to $x \to -\infty$.

Equation (8) can be simplified in several ways, such as by substituting for $\partial v/\partial t$ from the momentum equation so that $\partial \Gamma/\partial t$ is expressed entirely in terms of velocity components. Another approach is to integrate equation (8) in time, giving

$$\Gamma(t) = \frac{1}{2} \int_0^t u_{cl}^2(\tau) \, \mathrm{d}\tau + \frac{1}{\rho} \int_0^t \tilde{p}_{cl}(\tau) \, \mathrm{d}\tau - \int_0^{D/2} v(t, r)|_{x=0} \, \mathrm{d}r. \tag{9}$$

If only the total circulation ejected into the flow is of interest, then the upper limit of integration can be taken to be $t^* > t_p$ where t^* is sufficiently large so that $v(t^*, r) \approx 0$ over the nozzle. That is, for $t > t^*$, the vorticity has convected away from the nozzle exit plane under self-induction. Thus, equation (9) gives the total circulation ejected during the piston motion, Γ_T, as

$$\Gamma_T \equiv \Gamma(t^*) = \Gamma_U + \Gamma_p, \tag{10}$$

where

$$\Gamma_U \equiv \frac{1}{2} \int_0^{t_p} u_{cl}^2(t) \, \mathrm{d}t \tag{11}$$

is a vorticity flux term and

$$\Gamma_p \equiv \frac{1}{\rho} \int_0^{t^*} \tilde{p}_{cl}(t) \, \mathrm{d}t = \frac{1}{\rho} \int_0^{t^*} [p_{cl}(t) - p_\infty] \, \mathrm{d}t \tag{12}$$

is a term arising from over-pressure at the jet exit plane.

Equation (10) holds for both nozzle and orifice configurations. The only assumptions required to achieve this result are axisymmetry and negligible diffusion of vorticity across the nozzle centreline during vortex-ring formation (equation (7)). (The slug model also implicitly uses the assumption in equation (7). Didden (1979) apparently recognized that the diffusion of vorticity across the centreline could play a role, but estimated its effect to be negligible in his experiment.) The slug model can be obtained from equation (10) under the additional assumptions $u_{cl}(t) \approx U_J(t)$ and $\tilde{p}_{cl}(t) \approx 0$. The latter makes clear that the slug model ignores pressure effects during vortex-ring formation. The former also requires ignoring over-pressure during flow initiation, as will be demonstrated later.

The appearance of a pressure term in the equation for total circulation can be directly related to the appearance of axial gradients in the radial velocity as the ring is forming. Using a line integral of the momentum equation (see the Appendix), it can be shown that

$$\Gamma_p \approx \int_0^{t^*} \int_0^{D/2} \left(u \frac{\partial v}{\partial x} \right) \Bigg|_{x=0} \mathrm{d}r \, \mathrm{d}t \tag{13}$$

for negligible viscous effects. So, ignoring Γ_p is (approximately) equivalent to the parallel flow assumption used in deriving the slug-model. Conversely, accounting for over-pressure should correct the constant error in the slug-model predictions previously attributed to the parallel-flow assumption. The physical interpretation of the connection between $\partial v/\partial x$ and Γ_p is that nozzle exit over-pressure during initiation of the piston motion causes the jet fluid to accelerate radially as it is ejected, generating a $\partial v/\partial x$ component (streamline curvature) that contributes to vorticity flux and hence, to circulation.

3. A circulation model for the nozzle configuration

Based on equation (10), it is necessary only to model the conditions on the centreline at the nozzle exit plane to determine the total circulation. To provide improvements over the slug model, both Γ_p and u_{cl} must be modelled, especially during the start-up process. Most practical applications and vortex-ring investigations using a piston–cylinder mechanism involve a rapid start-up process with the jet velocity accelerating to a maximum velocity U_0 in a short time t_0 such that

$$\frac{1}{D} \int_0^{t_0} U_J(t) \, \mathrm{d}t < 1.$$

Following the initial start-up, the jet velocity remains at U_0 until pulse termination. This type of velocity program will be referred to as a nearly impulsive velocity program (NIVP), which reduces to an impulsive velocity program (IVP) in the limit $t_0 \to 0$. The following analysis will focus on NIVPs.

3.1. *A model for* Γ_p

For NIVPs, it is expected that over-pressure dominates during the initial phase of the piston motion when elevated pressure is required to rapidly accelerate the fluid in front of the nozzle. This is confirmed by the previous observation that Γ_p is related to $\partial v/\partial x$, which was shown by Didden (1979) to provide a significant contribution to the total circulation only during the initial flow acceleration (i.e. up to a time t_a sligthly longer than t_0). To determine a model for Γ_p, therefore, it is neccessary only to consider the flow initiation process, $0 < t < t_a$. During initiation, the flow is

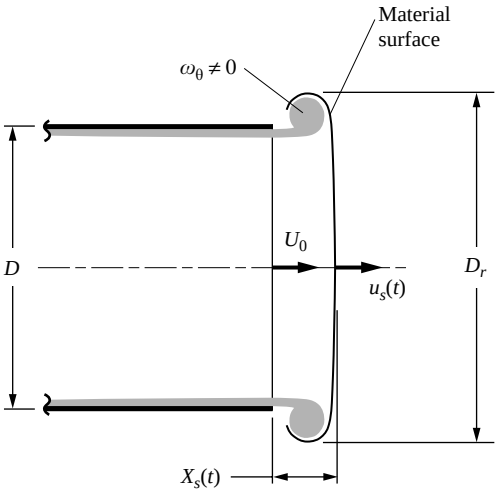

FIGURE 3. Flow shortly after initiation ($t = t_a$) for a nozzle configuration. The material surface was coincident with the nozzle exit plane at $t = 0$.

irrotational on the centreline and $\tilde{p}_{cl}$ can be determine using potential flow analysis. Integrating the unsteady form of Bernoulli's equation gives

$$\Gamma_p \approx \frac{1}{\rho}\int_0^{t_a} \tilde{p}_{cl}\,\mathrm{d}t = -\phi_{cl}|_{t_a} - \frac{1}{2}\int_0^{t_a} u_{cl}^2\,\mathrm{d}t = -\phi_{cl}|_{t_a} - O(U_0 L_a), \tag{14}$$

where $L_a = \int_0^{t_a} U_J(t)\,\mathrm{d}t$ and ϕ_{cl} is the velocity potential at $(x, r) = (0, 0)$.

The value of ϕ_{cl} at t_a is determined by the flow external to the nozzle after flow initiation, which is illustrated schematically in figure 3. Irrotationality along the centreline requires $u = \partial\phi/\partial x$, which integrates to

$$\phi_{cl}|_{t_a} = \phi_s - \int_0^{X_s} u\,\mathrm{d}x = \phi_s - O(U_0 X_s), \tag{15}$$

where ϕ_s is the velocity potential on the centreline at the material surface in figure 3. Owing to the rapid flow initiation, the front of the material surface is nearly flat (Nitsche 1996). Hence, downstream of this surface, the flow field is similar to potential flow in front of a disk of radius D_r translating at u_s. From the solution for the translating disk geometry,

$$\phi_s \approx -\frac{u_s D_r}{\pi} \tag{16}$$

(Batchelor 1967, §6.8; Saffman 1992, §6.4). For NIVPs and IVPs, however, $D_r/D \approx 1 + K_1(L_a/D)^{2/3}$ (Didden 1979; Nitsche 1996). Similarly, using this result with conservation of mass (assuming negligible entrainment by the ring at this early stage), it can be shown that $X_s/L_a \approx 1 - K_2(L_a/D)^{2/3}$ and $u_s/U_0 \approx 1 - K_3(L_a/D)^{2/3}$. Combining these results with equations (14)–(16) indicates that

$$\frac{\Gamma_p}{U_0 D} \approx \frac{1}{\pi}\left(1 - O\left(\frac{L_a}{D}\right)^{2/3}\right). \tag{17}$$

Thus, a reasonable model for NIVPs (small L_a/D) is $\Gamma_p/(U_0 D) \approx 1/\pi$.

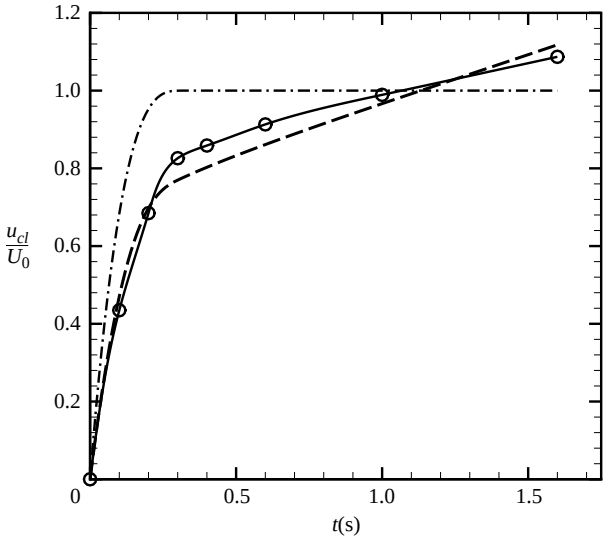

FIGURE 4. Centreline velocity data for the nozzle configuration of Didden (1979) compared with the pressure-corrected model for the centreline velocity and the slug model. ○, experiment (Didden 1979); —·—, $U_J(t)/U_0$ (slug model); – – –, pressure-corrected model.

$\frac{L}{D}$	$\frac{\Gamma_U}{U_0 D}$	$\frac{\Gamma_p}{U_0 D}$	$\frac{\Gamma_p}{\Gamma_U}$
0.6	0.20	0.29	1.44
1.0	0.39	0.34	0.87
1.4	0.61	0.34	0.56

TABLE 1. Measurements of Γ_U and Γ_p obtained from the data of Didden (1979).

It is important to realize that modelling Γ_p by equation (17) ignores the contribution to Γ_p that occurs when the piston is suddenly stopped at $t = t_p$. This contribution is negative and appears as a stopping vortex that travels back into the nozzle (as illustrated in the late-time dye visualization of Didden (1979) and Weigand & Gharib (1997)). Since the stopping vortex is not entrained by the ring, and the interest is in the vortex ring circulation, the contribution to Γ_p at pluse termination may be safely ignored. That is, Γ_T is taken as the total circulation outside the vortex-ring generator after the piston motion has stopped and the formation process is complete. (Ignoring the contribution to Γ_p from the piston deceleration when determining Γ_T may not be possible for short pulses ($L/D \ll 1$) since the forming vortex ring may not be far enough away from the jet exit plane at the termination of piston motion to avoid interaction between the forming vortex ring and the termination process in this limit).

The results of Didden (1979) provide a useful test of the proposed model for Γ_p for the nozzle configuration. Didden measured Γ_T and u_{cl} directly using laser-Doppler anemometry (LDA). The u_{cl} measurements (which are reproduced in figure 4) can be used to compute Γ_U using equation (11) and a piece-wise polynomial fit of the data. The estimated uncertainty in $\Gamma_U/(U_0 D)$ determined this way is ± 0.03. With Γ_U and Γ_T known, Γ_p is given by equation (10) as $\Gamma_p = \Gamma_T - \Gamma_U$. The results are shown in table 1.

Comparing the results for $\Gamma_p/(U_0 D)$ with the model value of $1/\pi = 0.32$ shows that the model agrees with the measured values to within the uncertainty in the measurements. This is remarkably good agreement considering the model validity is $O(L_a/D)^{2/3}$. The accuracy is accounted for to some degree by the fact that higher-order terms in the expansion tend to cancel. It is also worth noting that Γ_p can easily dominate the contribution to total circulation for $L/D < 1$, as illustrated by the results for Γ_p/Γ_U. The proposed model for Γ_p can therefore be very significant when thin vortex rings are considered.

3.2. *A model for* u_{cl}

Whereas Γ_p was modelled based on the flow external to the nozzle, u_{cl} is determined from the flow solution inside the nozzle. Assuming a thin boundary layer, the velocity potential inside the nozzle ($x \leqslant 0$) has the form

$$\phi(x, r, t) = U_c(t)x + \phi'(x, r, t), \tag{18}$$

where U_c is the uniform core velocity outside the boundary layer for an infinitely long pipe and ϕ' is the correction to the infinite pipe solution required near the nozzle exit.

The boundary conditions for ϕ' away from the nozzle exit are $[\partial\phi'/\partial x]_{x\to-\infty} = 0$ and $[\partial\phi'/\partial r]_{r=0,D/2} = 0$. At the nozzle exit, the boundary condition is determined by the external flow. Motivated by the model for Γ_p, $\phi'|_{x=0}$ at early time is approximated as the velocity potential in front of a disk of diameter $D = 2R$ translating at u_{cl}, namely,

$$\phi'|_{\substack{t\to 0\\ x=0}} \approx \phi_{disk}(r, t) = -\frac{2u_{cl}(t)}{\pi}\sqrt{R^2 - r^2} \tag{19}$$

(Batchelor 1967, §6.8; Saffman 1992, §6.4). At late time the forming ring translates away from the nozzle and the exit flow approaches a steady jet, which has a potential $\phi_{jet}(t)$ across the nozzle. Since the actual flow transitions between these two cases, the exit boundary condition on ϕ' is taken as

$$\phi'|_{x=0} = (1 - \sigma_n(t))\phi_{disk} + \sigma_n(t)\phi_{jet}, \tag{20}$$

where $0 \leqslant \sigma_n(t) \leqslant 1$ and $\sigma_n(t) \to 1$ at large time.

The resulting solution for the axial flow in the nozzle is

$$u = U_c - (1 - \sigma_n)\frac{2u_{cl}}{\pi}\sum_{k=0}^{\infty} A_k\delta_k \exp(\delta_k(x/R))J_0\left(\delta_k\frac{r}{R}\right), \tag{21}$$

where δ_k are the zeros of J_1 with $\delta_0 \equiv 0$, J_0 and J_1 are Bessel functions of the first kind of order 0 and 1, respectively, $A_0 = 2/3$, and

$$A_k = 2\frac{\sin(\delta_k) - \delta_k\cos(\delta_k)}{\delta_k^3 J_0^2(\delta_k)} \tag{22}$$

for $k > 0$. Solving (21) for u_{cl} gives

$$u_{cl}(t) = \frac{U_c(t)}{1 + 0.595(1 - \sigma_n(t))} \tag{23}$$

for a nozzle configuration.

As defined, the core velocity U_c is obtained from the boundary-layer solution in an infinitely long pipe. Assuming uniform flow outside the growing boundary layer, Shusser *et al.* (2002) related U_c to U_J for an IVP using Stokes solution for starting flow on a flat plate (thin-boundary-layer assumption). Dabiri & Gharib (2004) later

corrected a numerical error in Shusser *et al.* (2002) to achieve

$$\frac{U_c}{U_J} = 1 + \frac{8}{\sqrt{\pi}}\sqrt{\frac{\nu t}{D^2}}. \tag{24}$$

A more accurate result can be obtained from the solution by Das & Arakeri (1998), which is exact for infinitely long pipes and trapezoidal piston velocity programs. In practice, there is no significant difference between equation (24) and the results of Das & Arakeri in predicting u_{cl} for velocity programs with short acceleration periods (NIVPs) and pulse durations sufficiently short to avoid violation of the thin-boundary-layer assumption ($L/D < 10$ for typical Re_0). Consequently, equation (24) will be used to relate U_c to U_J in the present model for u_{cl}.

Finally, $\sigma_n(t)$ must be specified to close the model. To select an appropriate function of time, it is observed that, as the ring is forming, its speed, W, is steadily increasing. When W is sufficiently large, the ring starts to convect away from the nozzle and a steady jet begins to emerge behind it. The velocity of the ring at this point is predicted remarkably well by the slug model to be $U_0/2$ (Mohseni & Gharib 1998). Didden (1979), on the other hand, experimentally measured the ring velocity as $W/U_0 = 0.42\sqrt{X_p(t)/D}$ where $X_p(t)$ is the piston displacement. Until Didden's measured W reaches $U_0/2$, a reasonable function for $\sigma_n(t)$ is the ratio of these results, $\sigma_n(t)$ becoming unity thereafter. Explicitly,

$$\sigma_n(t) = \begin{cases} 0.84\sqrt{X_p(t)/D}, & X_p(t)/D < 1.42, \\ 1, & X_p(t)/D \geqslant 1.42. \end{cases} \tag{25}$$

Combining equations (23)–(25) gives an equation for u_{cl} at the exit of a pipe, given the jet velocity U_J as specified by the piston motion. Because the model accounts for the over-pressure effects during flow initiation through the exit boundary condition (20), it will be referred to as the 'pressure corrected' model for u_{cl}. A comparison of the predicted and measured u_{cl} for the experiments of Didden (1979) is shown in figure 4 for $U_0 = 4.6\,\mathrm{cm\,s^{-1}}$ and $t_p = 1.6\,\mathrm{s}$. The slug-model result is shown as the dash-dot line for comparison. The model prediction shows good agreement over the pulse duration, with a slight under-prediction as the piston velocity approaches U_0 near $t = 0.3\,\mathrm{s}$. The slug model, on the other hand, significantly over estimates u_{cl} during the start-up transient, but then under predicts u_{cl} at large time after boundary-layer growth begins to dominate the flow. Figure 5 also shows the predicted velocity profile at the nozzle exit plane, obtained from equation (21), in comparison to the measurements of Didden (1979). Aside from the slight offset of the results at $t = 0.4\,\mathrm{s}$ (owing to the under-prediction of u_{cl} by the model), the pressure-corrected model accurately predicts the velocity profile outside the boundary layer. The agreement also demonstrates the previous claim that the peak in axial velocity near the nozzle lip (and concomitant reduction in velocity at the centreline) during flow initiation is related to nozzle exit over-pressure.

3.3. *Verification of the model predictions of Γ_T*

Comparison of the model results for Γ_p and u_{cl} with those of Didden (1979) confirms the basic validity of the model, but it is useful to evaluate its predictions of Γ_T over a wider range of conditions. This is accomplished in table 2 using the results from several investigations. In table 2, the total circulation predicted using the model results is referred to as the pressure-corrected circulation, Γ_{pc}. The percentage error for the pressure-corrected and slug models is shown in the columns adjacent to the

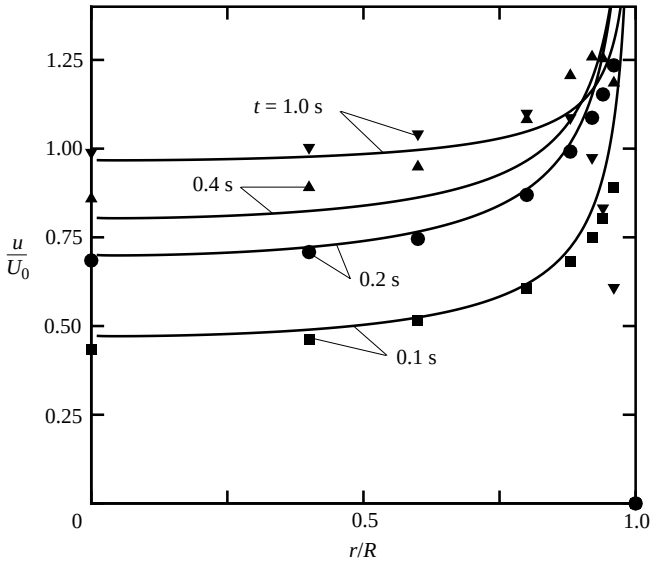

FIGURE 5. Comparison of axial velocity profiles at the nozzle exit as measured by Didden (1979) (symbols) and predicted by the pressure-corrected model (lines).

Source	$\frac{L}{D}$	Velocity program	α (deg.)	Re_0	$\frac{\Gamma_T}{U_0 D}$	$\frac{\Gamma_{pc}}{U_0 D}$	Error (%)	$\frac{\Gamma_{sm}}{U_0 D}$	Error (%)
Didden (1979)	0.6	NIVP[1]	20	2050	0.49	0.50	2.1	0.29	−42
	1.0				0.73	0.68	−6.2	0.48	−34
	1.4				0.96	0.91	−4.9	0.68	−29
	1.8				1.19	1.17	−1.7	0.88	−25
	2.2				1.37	1.42	3.9	1.08	−21
Weigand & Gharib (1997)	0.68	Trapezoidal[2]	20	1550	0.52	0.53	1.6	0.30	−41
				1770	0.51	0.52	2.7	0.30	−42
				1980	0.50	0.52	5.6	0.30	−40
				2170	0.49	0.51	4.9	0.30	−40
				2730	0.42	0.51	20	0.28	−33
				3620	0.42	0.49	17	0.26	−37
Rosenfeld *et al.* (1998)	6	IVP	0	2500	3.98	4.07	2.3	3.00	−25

[1]Didden (1979) used a nonlinear, smooth ramp up to U_0. The piston displacement during the acceleration period was $0.21D$.
[2]A trapezoidal velocity program is initiated with a linear ramp up to U_0 and terminated with a linear ramp down to zero velocity. In Weigand & Gharib (1997), the acceleration and deceleration periods corresponded to a piston displacement between 0.10 D ($Re_0 = 1550$) and 0.23 D (for $Re_0 = 3620$).

TABLE 2. Comparison of actual and predicted circulation for the nozzle configuration.

predicted values for each. Aside from the two high-Reynolds-number results from Weigand & Gharib (1997), the pressure-corrected model is accurate to within 6.2 %, including both large and small L/D and a range of Re_0. The slug model, on the other hand, under-predicts the total circulation between 21 % and 42 % (even for the relatively large L/D case of Rosenfeld *et al.* 1998). Didden (1979) and Weigand &

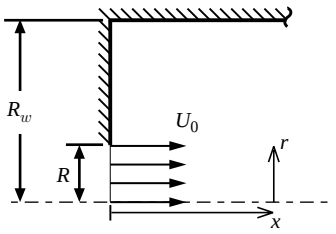

FIGURE 6. Domain geometry for determining ϕ_s in the orifice configuration.

Gharib (1997) do not report uncertainty in their measurements of circulation. The value reported by Rosenfeld *et al.* (1998), however, is estimated to be 1.2 % too low based on their mesh and time-step refinement studies.

The cause for the larger error of the pressure-corrected model at the two highest Re_0 cases in Weigand & Gharib (1997) is related to the velocity program. Weigand & Gharib used a trapezoidal program with fixed acceleration/deceleration times and constant L/D. As U_0 was increased to elevate Re_0, the velocity program became increasingly triangular. At the two highest Re_0 cases, the pressure-corrected model predicts that u_{cl} is still well below U_0 by the time the piston starts to decelerate. Thus, the flow starts to shut down before t_a is reached and the model over predicts Γ_p. Modifying the model for Γ_p to $\Gamma_p \approx u_{cl,max} D/\pi$, with $u_{cl,max}$ determined from the pressure-corrected model, reduces the error to 9.1 % and 4.9 % for $Re_0 = 2730$ and 3620, respectively.

4. A circulation model for the orifice configuration

The orifice configuration (figure 1) is distinctly different from the nozzle configuration owing to the large contraction experienced by the flow as it approaches the orifice and the planar boundary behind the flow after it exits. A realistic model for vortex-ring circulation generated by such a device must account for its distinct geometry. In the following, $D_p/D \to \infty$ is assumed in order to simplify the geometry as much as possible while still providing realistic results.

4.1. *A model for* Γ_p

A model for Γ_p in an orifice configuration can be obtained using the same reasoning as § 3.1. For rapid piston acceleration (NIVP), this gives $\Gamma_p \approx -\phi_s$. Whereas ϕ_s was approximated, to highest order, by the solution for a disk of diameter D moving through an infinite medium at U_0 for the nozzle configuration, the presence of the wall must be accounted for in the orifice configuration. For small L_a/D, the material surface in front of the forming ring is nearly coincident with the orifice exit plane and the configuration of interest for determining ϕ_s is as depicted in figure 6 for $R/R_w \to 0$.

The boundary conditions for the domain in figure 6 are $[\partial\phi/\partial r]_{r=0,R_w} = 0$, $[\partial\phi/\partial x]_{x\to\infty} = U_0(R/R_w)^2$ (by conservation of mass), and

$$\left.\frac{\partial\phi}{\partial x}\right|_{x=0} = \begin{cases} 0, & R < r \leqslant R_w, \\ U_0, & 0 \leqslant r \leqslant R. \end{cases} \tag{26}$$

In anticipation of taking $R/R_w \to 0$, the boundary condition at $x \to \infty$ is approximated as $[\partial\phi/\partial x]_{x\to\infty} \approx 0$. Using these boundary conditions, the solution for the velocity potential is obtained as

$$\phi(x, r) = -U_0 D \sum_{k=1}^{\infty} B_k \exp(-\delta_k (x/R_w)) J_0\left(\delta_k \frac{r}{R_w}\right), \tag{27}$$

where

$$B_k = \frac{J_1\left(\delta_k \dfrac{R}{R_w}\right)}{\delta_k^2 J_0^2(\delta_k)}. \tag{28}$$

Then, $\phi_s \approx \lim_{R/R_w \to 0} \phi(0,0) = -0.500(U_0 D)$. With this result, the pressure contribution to circulation for the orifice configuration is modelled as $\Gamma_p/(U_0 D) \approx 0.5$. Unlike the nozzle configuration, $D_r/D \approx 1$ to highest order for the orifice configuration (Pullin 1979), so the present model for $\Gamma_p/(U_0 D)$ is valid to $O(L_a/D)$.

4.2. *A model for* u_{cl}

Determining a model for u_{cl} is facilitated by the fact that both the early and late-time behaviour is known for the orifice configuration. The early-time velocity profile at the orifice is known from the potential flow solution through an orifice in an infinite plate. This result predicts $u_{cl} = U_J/2$ at flow initiation (Milne-Thomson 1968, § 16.56). For a long duration NIVP, a steady jet is approached as time proceeds and the vortex ring convects away from the exit plane. Because of the large contraction as the flow passes through the orifice, the jet continues to contract past the exit plane until the *vena contracta* is reached. The resulting streamline curvature at the orifice exit plane indicates that $\tilde{p}_{cl} > 0$, which also contributes to the flux of circulation by equation (10). Applying Bernoulli's equation between the exit plane and the *vena contracta*, the additional pressure contribution to circulation at long time can be accounted for by replacing u_{cl} with the jet velocity at the *vena contracta*, U_{vc}, in the expression for Γ_U. The velocity at the *vena contracta* is determined by $U_{vc} = U_J/C_c$, where C_c is the coefficient of contraction. The contraction coefficient is a function of Re_0 (for submerged jets) and the orifice lip geometry.

To account for the transition between the start-up and steady-jet conditions as time progresses, u_{cl} is modelled as

$$u_{cl} = \frac{U_J}{2 + (C_c - 2)\sigma_o(t)}, \tag{29}$$

where $0 \leqslant \sigma_o(t) \leqslant 1$ and $\sigma_o(t) \to 1$ at large time similar to $\sigma_n(t)$ for the nozzle case. It is emphasized that at large time, equation (29) gives an effective velocity appropriate for determining total circulation, not the actual centreline velocity at the exit plane. It is desirable to base the transition parameter $\sigma_o(t)$ on the ring velocity during formation as was done for the nozzle case, but, to the knowledge of the author, this has not been studied for the orifice case with large pulse duration ($L/D > 1$). An alternative option is to correct equation (25) for the orifice geometry. In this regard, the proper scaling of W depends on the jet velocity and diameter at the *vena contracta*, as opposed to the orifice exit plane. Making this correction gives

$$\sigma_o(t) = \begin{cases} \dfrac{0.84}{C_c^{3/4}}\sqrt{\dfrac{X(t)}{D}}, & X(t)/D < 1.42 C_c^{3/2}, \\ 1, & X(t)/D \geqslant 1.42 C_c^{3/2}, \end{cases} \tag{30}$$

where $X(t) = (D_p/D)^2 X_p(t)$ is the length of the fluid slug ejected from the orifice at time t.

4.3. *Verification of the model predictions of* Γ_T

The availability of circulation measurements for vortex rings generated by an orifice configuration is limited, despite the recent interest in synthetic jet actuators (many

$\frac{L}{D}$	Re_0	$\frac{\Gamma_T}{U_0 D}$	$\frac{\Gamma_{pc}}{U_0 D}$	Error (%)	$\frac{\Gamma_{sm}}{\Gamma_0 D}$	Error (%)
1.33	2.04×10^4	2.03	1.77	−13	0.67	−67
1.33	2.65×10^4	1.96	1.77	−9.6	0.67	−66
1.33	2.94×10^4	2.04	1.77	−13	0.67	−67

TABLE 3. Comparison of predicted circulation for the orifice configuration with the results of Sallet (1975).

of which have a similar geometry). Sallet (1975) does, however, provide circulation measurements for vortex rings formed in air using an orifice configuration with $D_p/D = 2.0$. Sallet's conditions correspond to $Re_0 > 2 \times 10^4$, for which $C_c \approx 0.61$ if the nozzle lip is sharp (Vennard 1954). Using this C_c in the pressure-corrected model for the orifice configuration and comparing with Sallet (1975) gives the results in table 3. The acceleration and deceleration times used by Sallet were only a small fraction of the total pulse duration, so IVPs were assumed to obtain the model results in table 3. A comparison with the slug model is also presented in the last column.

The agreement between the pressure-corrected model and the measurements is good (within −13 %) for the limited number of cases available. This agreement is dramatically better than the slug model, which is only accurate to within −67 %. Nevertheless, the pressure-corrected model could easily be improved with a $\sigma_o(t)$ more directly tied to the geometry of interest.

The comparison between the pressure-corrected model and the measurements of Sallet (1975) should be viewed with some caution, however, since the ring circulation measurements were not direct measurements. Rather, the ring circulation was inferred from measurements of the ring core diameter and ring velocity using Oseen's solution for a line vortex. While the approach is approximately correct for thin vortex rings, it is not a direct circulation measurement such as would be available from digital particle-image velocimetry (DPIV). An additional concern is that the geometry of the orifice lip (rounded, sharp, square, etc.) can noticeably affect the vortex-formation process, as demonstrated by Shuster & Smith (2004) in the case of synthetic jets. Sallet (1975) does not give details of the orifice geometry, but it was assumed to be sufficiently sharp to use $C_c \approx 0.61$ in the pressure-corrected model. Nevertheless, it is clear the slug model is wholly inadequate for this geometry, and the pressure-corrected model provides a reasonable correction for predicting circulation.

5. Concluding remarks

The slug model presents a simple formula for estimating the circulation produced by a piston–cylinder vortex ring generator, but it consistently underestimates the actual circulation by a nearly constant amount for NIVPs. The error comes primarily from neglecting over-pressure that develops at the nozzle/orifice exit plane during flow initiation, which produces radial flow at the jet exit plane and deforms the axial velocity profile. Accounting for the radial flow contribution through a pressure term, Γ_p, in the equation for total circulation, a model for Γ_p is developed for both nozzle and orifice geometries. Pressure effects on the velocity profile at the nozzle/orifice exit plane were also accounted for in models for u_{cl} in both geometries to accurately determine the circulation flux term Γ_U. For the nozzle geometry, this resulted in an approximate solution for starting flow at the exit of an infinite pipe, which included

a boundary-layer correction for long-time behaviour. Total circulation predicted by both models agrees well with measurements, showing substantial improvement over the slug model. The exception is for velocity programs that are nearly triangular.

Notably, the discussion of the orifice configuration was significantly hampered, both in terms of modelling and verification, by the lack of experimental results. Aside from the theoretical work of Pullin (1979), which is valid only for the initial instants of piston motion, there has been no systematic comparison of vortex-ring formation by nozzle and orifice configurations. (James & Madnia 1996, among others, have compared nozzle and 'orifice' geometries, but the orifice geometry considered consisted of a pipe abutted with an infinite place, which eliminates the flow contraction approaching the orifice in a true orifice geometry.) Such a comparison would provide valuable information given the distinct differences between the two geometries, which is clearly evidenced by the dramatically worse performance of the slug model for the orifice case.

An additional issue that has been apparent throughout the discussion is a restriction to velocity programs with rapid initial piston accelerations. More gradually initiated flow is also of interest, in part because of the influence this difference has on the impulse supplied to the flow by a starting jet (Krueger & Gharib 2003). For gradually initiated flow, however, modelling the over-pressure is more complicated because over-pressure no longer dominates only at flow initiation and the development process of the ring becomes important. The precise conditions under which the details of the piston acceleration must be considered are not clear. For the cases considered herein, the acceleration phase was always completed before the ejected slug length had reached $1.0D$, resulting in the so-called 'nearly impulsive velocity program' (NIVP) where modelling the pressure effects only at initiation worked well. The total impulse results of Krueger & Gharib (2003) indicate that the impulse supplied by over-pressure decreases as the jet is initiated more gradually, which suggests the over-pressure correction to circulation should decrease as well. A more detailed model of the ring development is required to capture this trend in Γ_p.

The author wishes to acknowledge many helpful discussions with Professors Anthony Leonard, John Dabiri and Morteza Gharib during the preparation of this paper.

Appendix. The relationship between Γ_p and gradients in radial velocity

A relationship between Γ_p and the radial velocity component v can be obtained from a line integral of the momentum equation along the contour from $r = 0$ on the jet exit plane to $x = -\infty$ on the outer annulus of a nozzle configuration (segments 2 and 1 in figure 2). Explicitly,

$$\frac{1}{\rho}\int_{2+1}\nabla\tilde{p}\cdot\mathrm{d}\boldsymbol{c} = \int_{2+1}\left[-\frac{\mathrm{D}\boldsymbol{u}}{\mathrm{D}t} + \nu\nabla^2\boldsymbol{u}\right]\cdot\mathrm{d}\boldsymbol{c}. \tag{A 1}$$

For simplicity, $\alpha = 0$ will be assumed in the following. Integrating equation (A 1) with appropriate boundary conditions on the outer annulus gives,

$$-\frac{\tilde{p}_{cl}}{\rho} = \int_0^{D/2}\left\{-\left(\frac{\partial v}{\partial t} + \frac{1}{2}\frac{\partial v^2}{\partial r} + u\frac{\partial v}{\partial x}\right) + \nu\left[\frac{1}{r}\frac{\partial}{\partial r}\left(r\frac{\partial v}{\partial r}\right) + \frac{\partial^2 v}{\partial x^2} - \frac{v}{r^2}\right]\right\}\Bigg|_{x=0}\mathrm{d}r,$$
$$+\nu\int_0^{-\infty}\frac{1}{r}\frac{\partial}{\partial r}\left(r\frac{\partial u}{\partial r}\right)\Bigg|_{r=D/2}\mathrm{d}x, \tag{A 2}$$

where the last term is evaluated at $r = D/2$ on the outside of the nozzle. Simplifying with continuity, integrating total differentials, and integrating in time gives an expression for Γ_p entirely in terms of velocity components, namely,

$$\Gamma_p \equiv \int_0^{t^*} \frac{\tilde{p}_{cl}}{\rho}\,\mathrm{d}t = \underbrace{\int_0^{t^*}\int_0^{D/2} \left(u\frac{\partial v}{\partial x}\right)\bigg|_{x=0} \mathrm{d}r\,\mathrm{d}t}_{\text{I}} - \underbrace{\nu\int_0^{t^*} \frac{\partial u}{\partial x}\bigg|_{x,r=0} \mathrm{d}t}_{\text{II}}$$
$$- \underbrace{\nu\int_0^{t^*}\int_0^{D/2} \frac{\partial^2 v}{\partial x^2}\bigg|_{x=0} \mathrm{d}r\,\mathrm{d}t}_{\text{III}} - \underbrace{\nu\int_0^{t^*}\int_0^{-\infty} \frac{1}{r}\frac{\partial}{\partial r}\left(r\frac{\partial u}{\partial r}\right)\bigg|_{r=D/2} \mathrm{d}x\,\mathrm{d}t}_{\text{IV}}. \quad \text{(A 3)}$$

In obtaining this result it has been assumed that $[\partial u/\partial x]_{x=0,r=D/2} = 0$ in accordance with the no-slip boundary condition inside the nozzle, and it was observed that

$$\int_0^{t^*}\int_0^{D/2} \frac{\partial v}{\partial t}\bigg|_{x=0} \mathrm{d}r\,\mathrm{d}t = 0$$

by the definition of t^*.

The viscous terms (II, III and IV) in equation (A 3) are negligible compared to the convective term I for sufficiently high Reynolds number. This can be demonstrated by re-scaling the terms. For a piston velocity program that rapidly accelerates to a velocity U_0 and remains there for the duration of the pulse, the appropriate variable scalings over the nozzle at the exit plane are $u \sim U_0$, $x \sim U_0 t^*$ and $r \sim R = D/2$. Using these results in the continuity equation implies $v \sim R/t^*$. Hence, the magnitudes of terms II and III relative to term I scale as,

$$\frac{\text{Term I}}{\text{Term II}} \sim \frac{R^2}{\nu t^*} \sim \frac{Re_0}{L/D} \quad \text{(A 4)}$$

and

$$\frac{\text{Term I}}{\text{Term III}} \sim \frac{U_0^2 t^*}{\nu} \sim Re_0 \frac{L}{D}. \quad \text{(A 5)}$$

For term IV (which is evaluated outside the nozzle), the same u and r scaling is appropriate, but a more appropriate x scaling is $x \sim R$ since the viscous effect outside the nozzle is confined to a region near the exit plane. As a result,

$$\frac{\text{Term I}}{\text{Term IV}} \sim \frac{R^2}{\nu t^*}\frac{R}{U_0 t^*} \sim \frac{Re_0}{(L/D)^2} \quad \text{(A 6)}$$

(Note that term IV represents the entrainment of negative vorticity developed on the outer annulus of the nozzle during the initial stages of vortex-ring formation.)

The condition that vorticity diffusion across the centreline be negligible (equation (7)) combined with equation (A 4) indicates that term II is negligible compared to term I. Similarly, terms III and IV are negligible compared to term I provided equation (7) holds and L/D is $O(1)$. That is, under conditions very similar to those used to deduce $\Gamma_T = \Gamma_U + \Gamma_p$, equation (A 3) reduces to

$$\Gamma_p \approx \int_0^{t^*}\int_0^{D/2} \left(u\frac{\partial v}{\partial x}\right)\bigg|_{x=0} \mathrm{d}r\,\mathrm{d}t. \quad \text{(A 7)}$$

This result demonstrates that the contribution to circulation from pressure is directly related to the longitudinal gradient of v at $x = 0$ (i.e. streamline curvature at the

nozzle exit plane). Likewise, the assumption that $\partial v/\partial x = 0$ is the reason Γ_p does not appear in the slug-model result for circulation.

REFERENCES

Anderson, E. J. & Grosenbaugh, M. A. 2005 Jet flow in steadily swimming adult squid. *J. Exp. Biol.* **208**, 1125–1146.

Batchelor, G. K. 1967 *An Introduction to Fluid Dynamics*. Cambridge University Press.

Cantwell, B. J. 1986 Viscous starting jets. *J. Fluid Mech.* **173**, 159–189.

Dabiri, J. O. & Gharib, M. 2004 A revised slug model boundary layer correction for starting jet vorticity flux. *Theoet. Comput. Fluid Dyn.* **17**, 293–295.

Das, D. & Arakeri, J. H. 1998 Transition of unsteady velocity profiles with reverse flow. *J. Fluid Mech.* **374**, 251–283.

Didden, N. 1979 On the formation of vortex rings: rolling-up and production of circulation. *Z. Angew. Math. Phys.* **30**, 101–116.

Gharib, M., Rambod, E. & Shariff, K. 1998 A universal time scale for vortex ring formation. *J. Fluid Mech.* **360**, 121–140.

Glezer, A. 1988 The formation of vortex rings. *Phys. Fluids* **31**, 3532–3542.

Glezer, A. & Amitay, M. 2002 Synthetic jets. *Annu. Rev. Fluid Mech.* **34**, 503–529.

Heeg, R. S. & Riley, N. 1997 Simulations of the formation of an axisymmetric vortex ring. *J. Fluid Mech.* **339**, 199–211.

James, S. & Madnia, C. K. 1996 Direct numerical simulation of a laminar vortex ring. *Phys. Fluids* **8**, 2400–2414.

Krueger, P. S. & Gharib, M. 2003 The significance of vortex ring formation to the impulse and thrust of a starting jet. *Phys. Fluids* **15**, 1271–1281.

Krueger, P. S. & Gharib, M. 2005 Thrust augmentation and vortex ring evolution in a fully pulsed jet. *AIAA J.* **43**, 792–801.

Lim, T. T. & Nickels, T. B. 1995 Vortex rings. In *Fluid Vortices* (ed. S. I. Green). Kluwer.

Milne-Thomson, L. M. 1968 *Theoretical Hydrodynamics*. Dover.

Mohseni, K. & Gharib, M. 1998 A model for universal time scale of vortex ring formation. *Phys. Fluids* **10**, 2436–2438.

Nitsche, M. 1996 Scaling properties of vortex ring formation at a circular tube opening. *Phys. Fluids* **8**, 1848–1855.

Nitsche, M. & Krasny, R. 1994 A numerical study of vortex ring formation at the edge of a circular tube. *J. Fluid Mech.* **276**, 139–161.

Pullin, D. I. 1979 Vortex ring formation at tube and orifice openings. *Phys. Fluids* **22**, 401–403.

Rosenfeld, M., Rambod, E. & Gharib, M. 1998 Circulation and formation number of laminar vortex rings. *J. Fluid Mech.* **376**, 297–318.

Saffman, P. G. 1992 *Vortex Dynamics*. Cambridge University Press.

Sallet, D. W. 1975 Impulsive motion of a circular disk which causes a vortex ring. *Phys. Fluids* **18**, 109–111.

Shariff, K. & Leonard, A. 1992 Vortex rings. *Annu. Rev. Fluid Mech.* **24**, 235–279.

Shusser, M., Gharib, M., Rosenfeld, M. & Mohseni, K. 2002 On the effect of pipe boundary layer growth on the formation of a laminar vortex ring generated by a piston/cylinder arrangement. *Theoret. Comput. Fluid Dyn.* **15**, 303–316.

Shuster, J. M. & Smith, D. R. 2004 A study of the formation and scaling of a synthetic jet. *AIAA Paper* 2004-0090, *Proc. 42nd AIAA Aerospace Sci. Meeting and Exhibit*.

Siekmann, J. 1963 On a pulsating jet from the end of a tube, with application to the propulsion of certain aquatic animals. *J. Fluid Mech.* **15**, 399–418.

Vennard, J. K. 1954 *Elementary Fluid Mechanics*. John Wiley.

Weigand, A. & Gharib, M. 1997 On the evolution of laminar vortex rings. *Exps. Fluids* **22**, 447–457.

Weihs, D. 1977 Periodic jet propulsion of aquatic creatures. *Forsch. Zool.* **24**, 171–175.

Zhao, W., Frankel, S. H. & Mongeau, L. G. 2000 Effects of trailing jet instability on vortex ring formation. *Phys. Fluids* **12**, 589–596.